Electronic Supplementary Material (ESI) for RSC Advances.

Supporting Information

Lattice Reconstruction of Cs-Introduced $FAPbI_{1.80}Br_{1.20}$ Enables Improved Stability for Perovskite Solar Cells

Shuang Chen, Lu Pan, Tao Ye, Nuo Lei, Yijun Yang and Xi Wang*

Key Laboratory of Luminescence and Optical Information, Ministry of Education, Department of Physics, School of Science, Beijing Jiaotong University, Beijing, 100044, China.

* Corresponding author email: *xiwang@bjtu.edu.cn*.

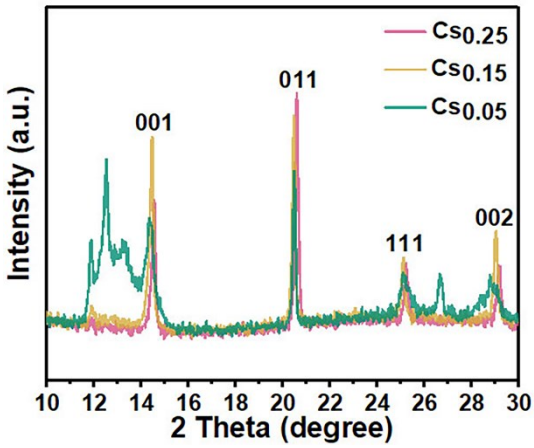

Fig. S1 XRD detail of $Cs_xFA_{1-x}PbI_{1.80}Br_{1.20}$ (x = 0.05, 0.15, 0.25) perovskite films.

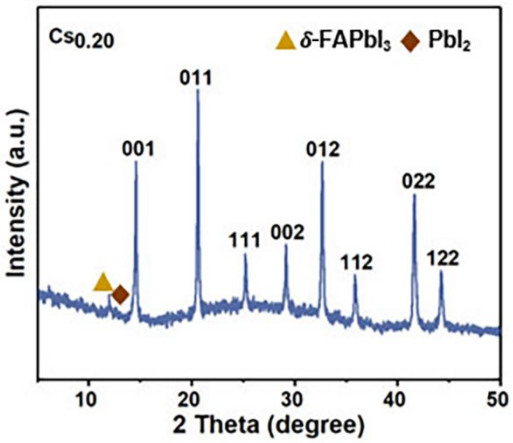

Fig. S2 XRD spectrum of $Cs_{0.20}FA_{0.80}PbI_{1.80}Br_{1.20}$ perovskite film.

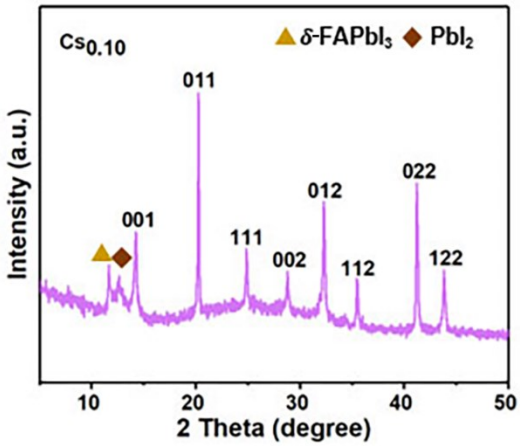

Fig. S3 XRD spectrum of $Cs_{0.10}FA_{0.90}PbI_{1.80}Br_{1.20}$ perovskite film.

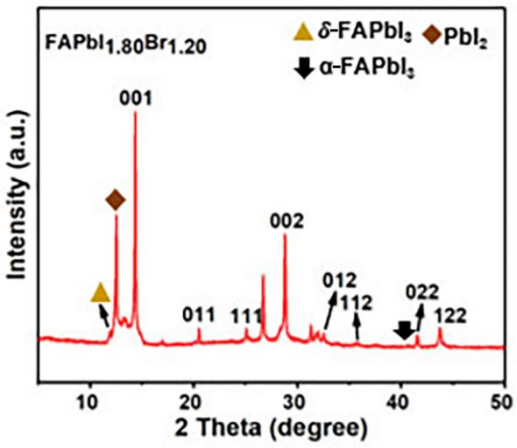

Fig. S4 XRD spectrum of $FAPbI_{1.80}Br_{1.20}$ perovskite film.

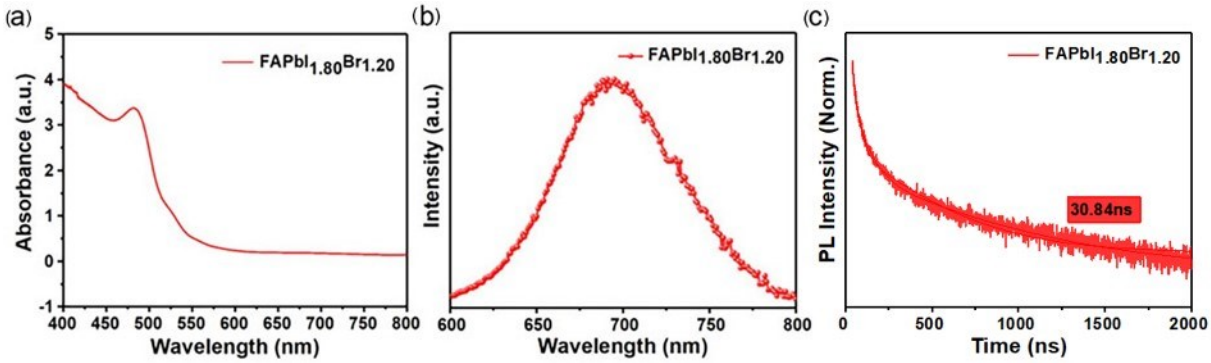

Fig. S5 Optical characterization of $FAPbI_{1.80}Br_{1.20}$. (a) Absorption spectrum of $FAPbI_{1.80}Br_{1.20}$ film. (b) Photoluminescence spectrum of $FAPbI_{1.80}Br_{1.20}$ film. (c) TRPL spectrum of $FAPbI_{1.80}Br_{1.20}$ film.

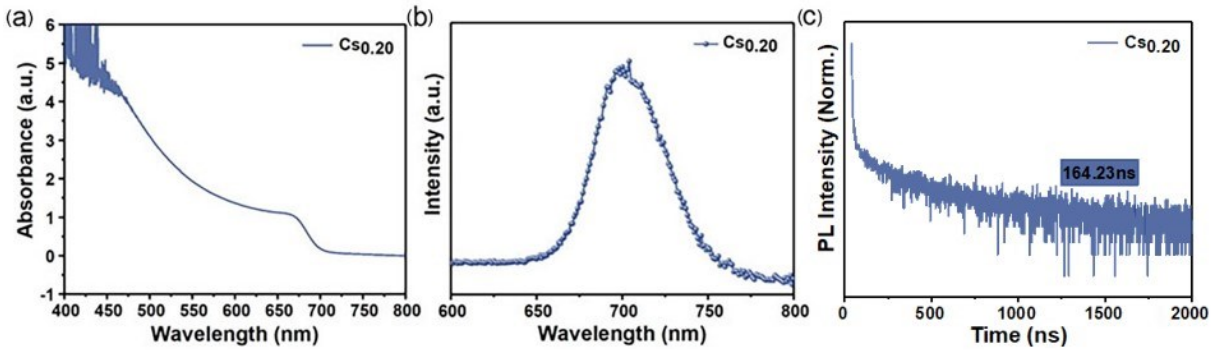

Fig. S6 Optical characterization of $Cs_{0.20}FA_{0.80}PbI_{1.80}Br_{1.20}$. (a) Absorption spectrum of $Cs_{0.20}FA_{0.80}PbI_{1.80}Br_{1.20}$ film. (b) Photoluminescence spectrum of $Cs_{0.20}FA_{0.80}PbI_{1.80}Br_{1.20}$ film. (c) TRPL spectrum of $Cs_{0.20}FA_{0.80}PbI_{1.80}Br_{1.20}$ film.

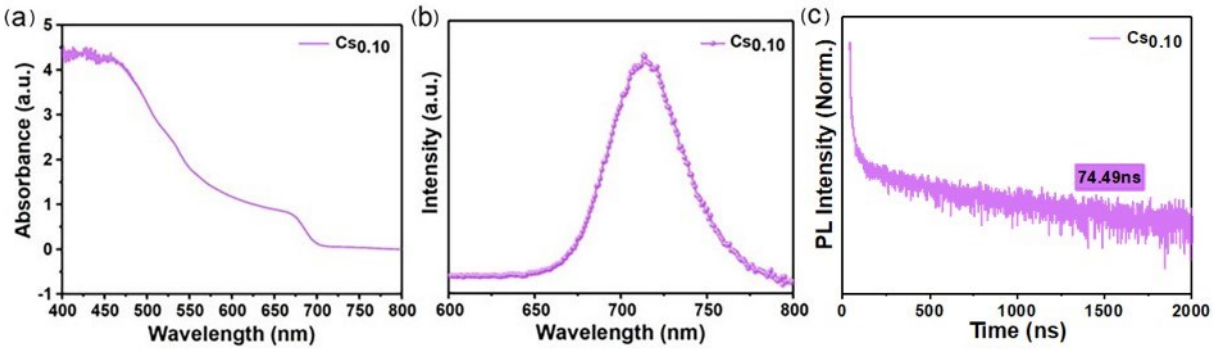

Fig. S7 Optical characterization of $Cs_{0.10}FA_{0.90}PbI_{1.80}Br_{1.20}$. (a) Absorption spectrum of $Cs_{0.10}FA_{0.90}PbI_{1.80}Br_{1.20}$ film. (b) Photoluminescence spectrum of $Cs_{0.10}FA_{0.90}PbI_{1.80}Br_{1.20}$ film. (c) TRPL spectrum of $Cs_{0.10}FA_{0.90}PbI_{1.80}Br_{1.20}$ film.

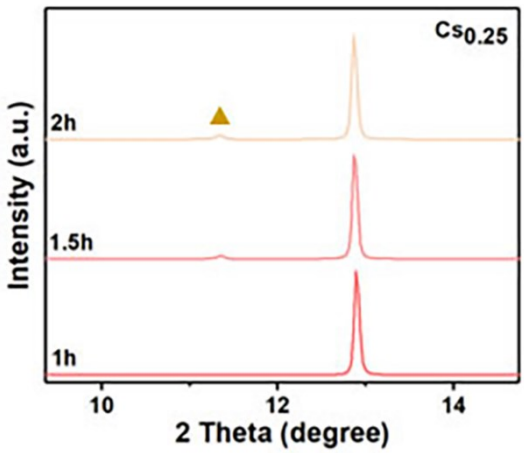

Fig. S8 Mixed-halide perovskite films heated on a 200 °C hotplate inside a N_2-filled glovebox for 2 hours. Zoom-in corresponding to the $Cs_{0.25}FA_{0.75}PbI_{1.80}Br_{1.20}$ perovskite films.

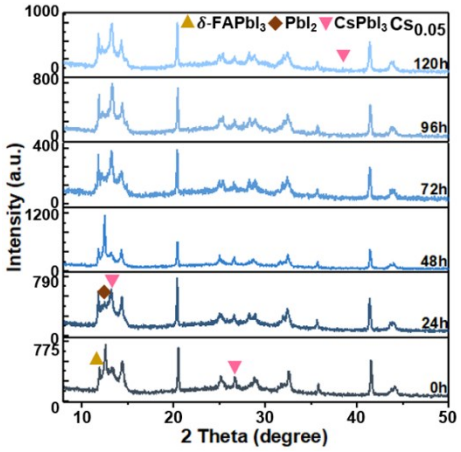

Fig. S9 Stability test (environmental condition 25 °C, 55-60% humidity). Zoom-in corresponding to the $Cs_{0.05}FA_{0.95}PbI_{1.80}Br_{1.20}$ perovskite films.

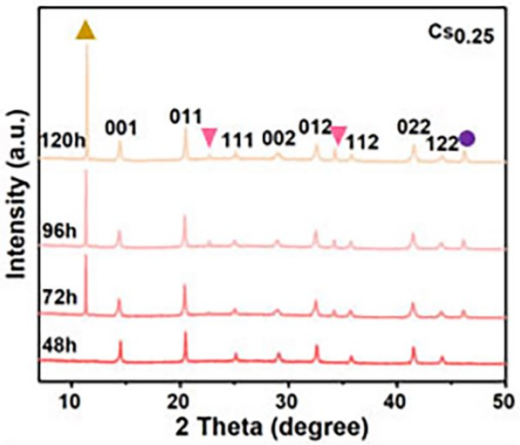

Fig. S10 Stability test (environmental condition 25 °C, 55-60% humidity). Zoom-in corresponding to the $Cs_{0.25}FA_{0.75}PbI_{1.80}Br_{1.20}$ perovskite films.

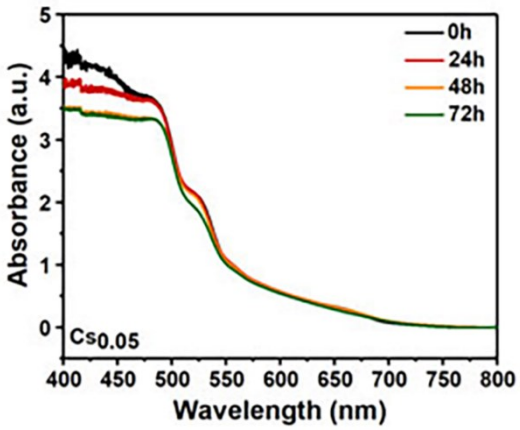

Fig. S11 Air stability and film formation dependence on processing conditions. UV-visible absorption of $Cs_{0.05}FA_{0.95}PbI_{1.80}Br_{1.20}$ films for 0 h, 24 h, 48 h, 72 h in wet.

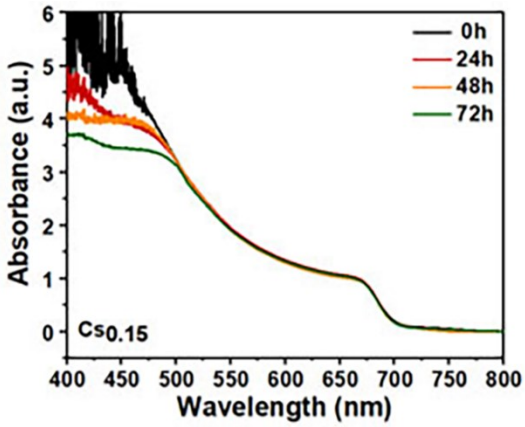

Fig. S12 Air stability and film formation dependence on processing conditions. UV- visible absorption of $Cs_{0.15}FA_{0.85}PbI_{1.80}Br_{1.20}$ films for 0 h, 24 h, 48 h, 72 h in wet.

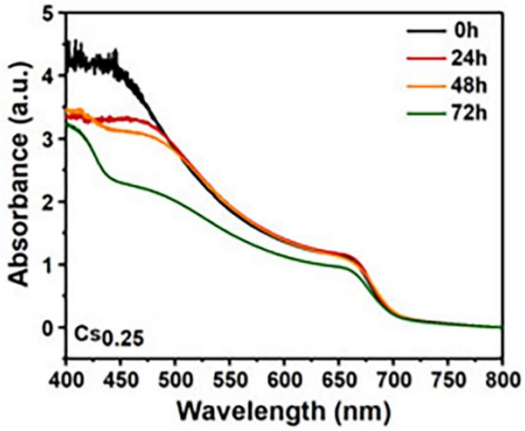

Fig. S13 Air stability and film formation dependence on processing conditions. UV- visible absorption of $Cs_{0.25}FA_{0.75}PbI_{1.80}Br_{1.20}$ films for 0 h, 24 h, 48 h, 72 h in wet.

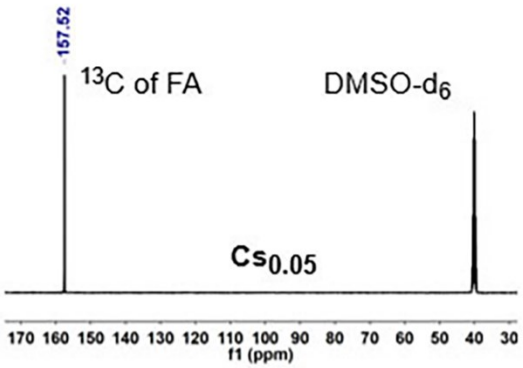

Fig. S14 Liquid-state ^{13}C-NMR spectrum of $Cs_{0.05}FA_{0.95}PbI_{1.80}Br_{1.20}$ precipitate powder in DMSO-d_6.

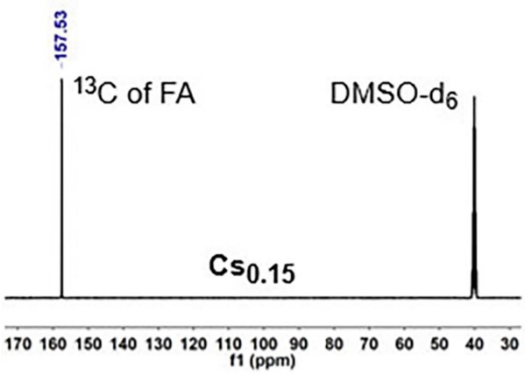

Fig. S15 Liquid-state ^{13}C-NMR spectrum of $Cs_{0.15}FA_{0.85}PbI_{1.80}Br_{1.20}$ precipitate powder in DMSO-d_6.

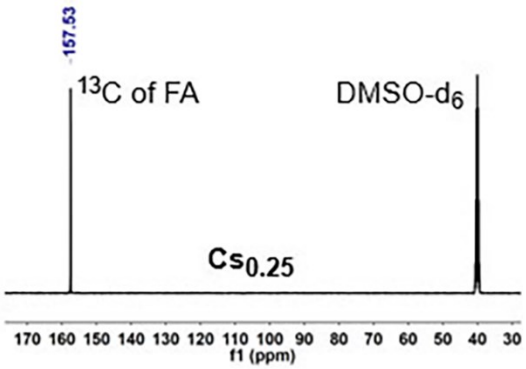

Fig. S16 Liquid-state ^{13}C-NMR spectrum of $Cs_{0.25}FA_{0.75}PbI_{1.80}Br_{1.20}$ precipitate powder in DMSO-d_6.

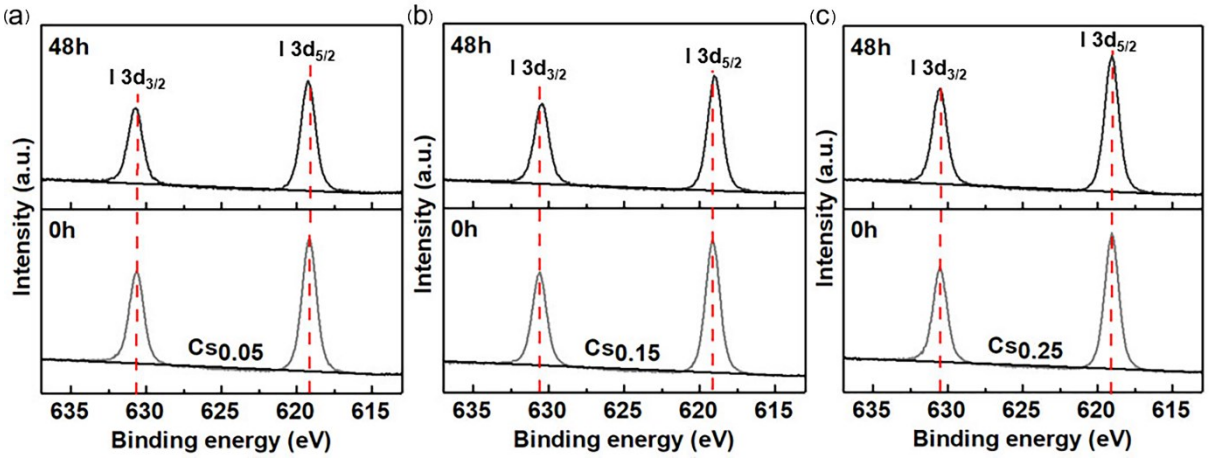

Fig. S17 Stability test (environmental condition 25 °C, 55-60% humidity). XPS spectra of I $3d_{3/2}$ and I $3d_{5/2}$ of $Cs_xFA_{1-x}PbI_{1.80}Br_{1.20}$ (x = 0.05, 0.15, 0.25) perovskite thin films in wet.

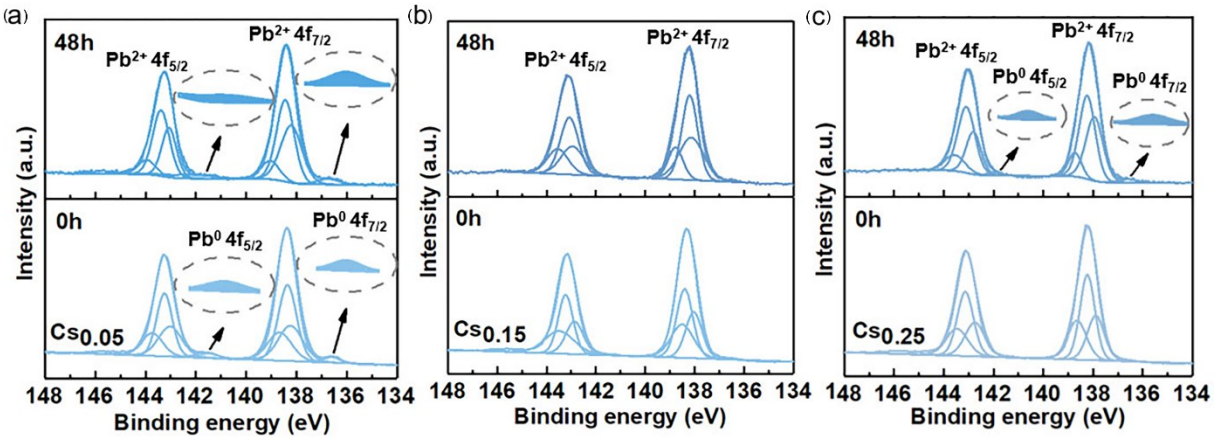

Fig. S18 Stability test (environmental condition 25 ℃, 55-60% humidity). XPS spectra of Pb $4f_{5/2}$ and Pb $4f_{7/2}$ of $Cs_xFA_{1-x}PbI_{1.80}Br_{1.20}$ (x = 0.05, 0.15, 0.25) perovskite thin films in wet.

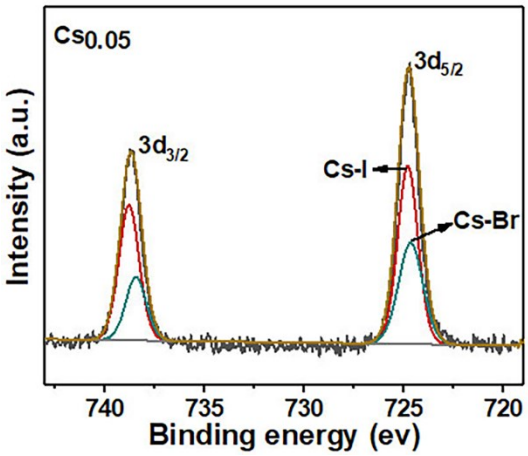

Fig. S19 XPS spectrum of Cs $3d_{3/2}$ and Cs $3d_{5/2}$ of $Cs_{0.05}FA_{0.95}PbI_{1.80}Br_{1.20}$ perovskite thin film.

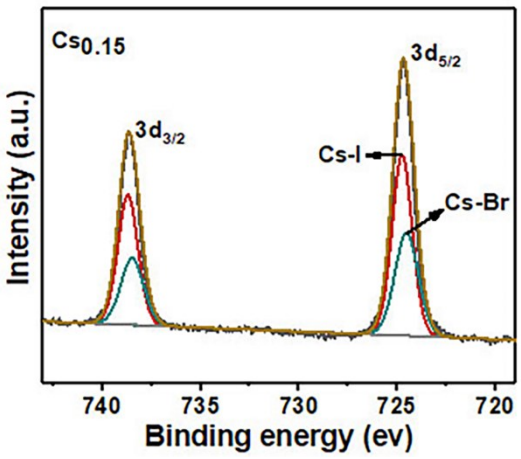

Fig. S20 XPS spectrum of Cs $3d_{3/2}$ and Cs $3d_{5/2}$ of $Cs_{0.15}FA_{0.85}PbI_{1.80}Br_{1.20}$ perovskite thin film.

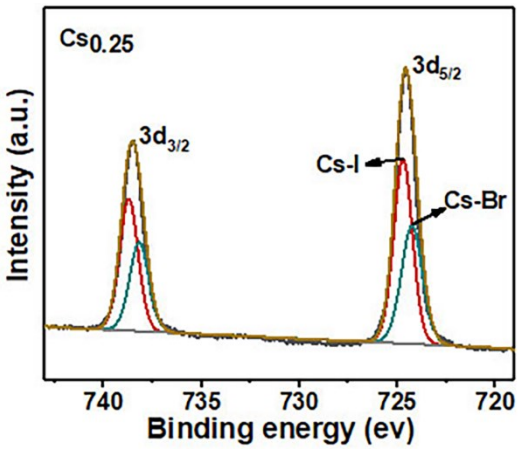

Fig. S21 XPS spectrum of Cs $3d_{3/2}$ and Cs $3d_{5/2}$ of $Cs_{0.25}FA_{0.75}PbI_{1.80}Br_{1.20}$ perovskite thin film.

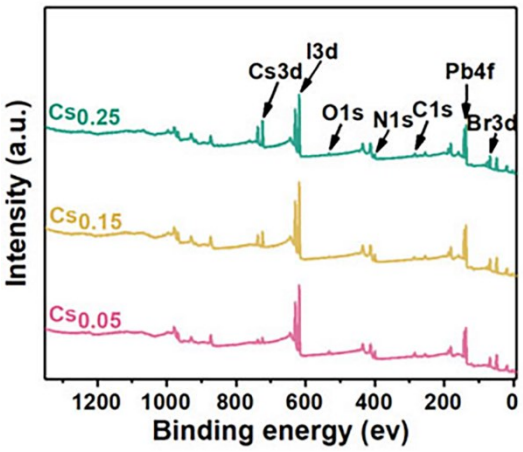

Fig. S22 XPS spectra for different Cs/FA ratio mixed cation thin films.

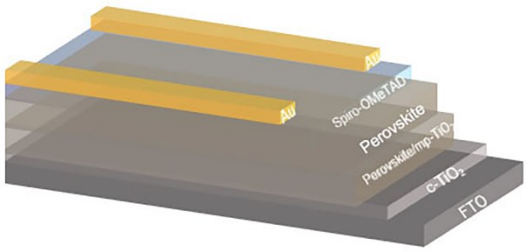

Fig. S23 Device structure of PSCs with glass/FTO/c-TiO2/mp-TiO2/perovskite/Spiro-OMeTAD/Au.

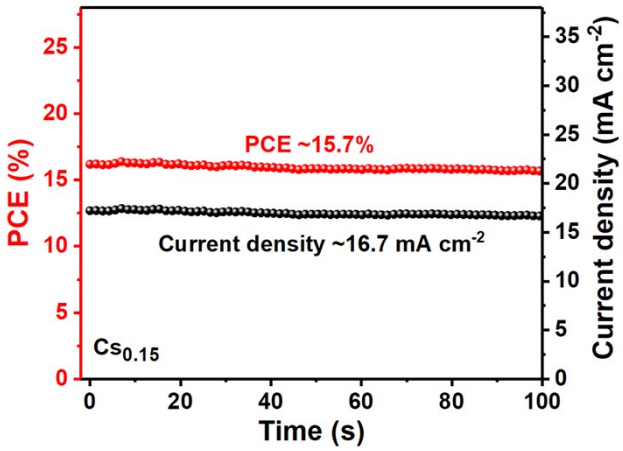

Fig. S24 Steady-state PCE and current density of the champion device ($Cs_{0.15}$) measured at maximum-power point of 0.86 V.

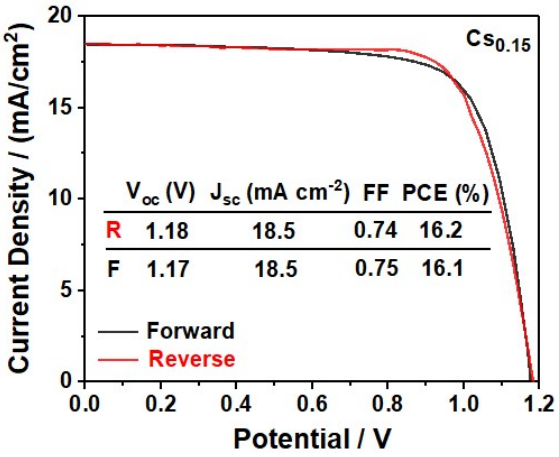

Fig. S25 J-V curves of the champion device ($Cs_{0.15}$) in reverse and forward scan directions.

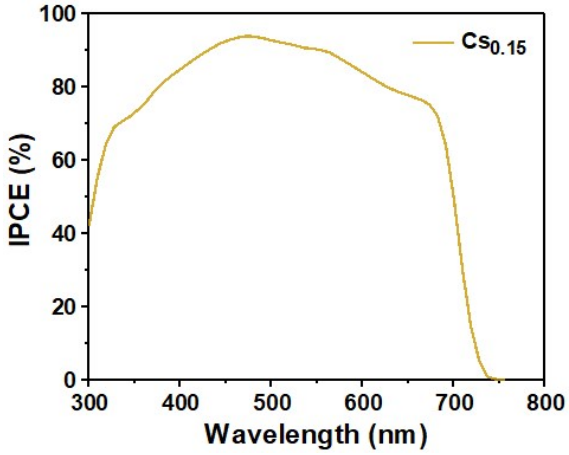

Fig. S26 Incident-photon-to-current-efficiency (IPCE) spectrum of 15% Cs+ incorporated PSCs.

Table S1 TRPL results. The obtained carrier lifetimes of $Cs_xFA_{1-x}PbI_{1.80}Br_{1.20}$ (x = 0, 0.10, 0.20) perovskite films.

Perovskite	A_1 (%)	τ_1 (ns)	A_2 (%)	τ_2 (ns)	Lifetime (ns)
$Cs_{0.20}FA_{0.80}PbI_{1.80}Br_{1.20}$	33.44	2.05	10.0	170.74	164.23
$Cs_{0.10}FA_{0.90}PbI_{1.80}Br_{1.20}$	91.34	2.82	10.03	94.06	74.49
$FAPbI_{1.80}Br_{1.20}$	16.24	12.94	1.19	73.71	30.84